Trabajo Fin de Grado en Física

Interaction of bioactive molecules with model membranes using Langmuir monolayers

María Pedrosa Bustos
Universidad de Granada
Julio de 2018

UNIVERSIDAD
DE GRANADA

Tutoras: María José Gálvez Ruiz y Julia Maldonado Valderrama
Departamento de Física Aplicada
Universidad de Granada

Abstract

This Final Degree Project presents a study on the interaction between an anti-cancer drug model, curcumin, and two experimental monolayers at the air-water interface modeling tumor and normal cell membrane systems. The analysis is perform by means of the Langmuir monolayer technique, where the surface pressure-area isotherms obtained by compressing the films are recorded. In the first place and in order to learn the experimental procedure and test the efficacy of the method, the widely studied pure monolayers of cholesterol (Chol), sphingomyelin (Sph) and DDPC are characterized, obtaining results that agree with literature. Subsequently, Chol:DDPC and Chol:Sph mixed monolayers modeling healthy and cancerous cell membranes are created and analyzed, concluding that the addition of cholesterol to pure monolayers condenses the system. Finally, curcumin where added in different different amounts to both models. The study of certain important thermodynamic parameters, such as the excess free energy ΔG_{exc} and the excess surface area A_{exc}, revealed that curcumin penetrates more into the tumor membrane model, supporting the use of this drug in studies aimed at the creation of smart anticancer drugs.

Resumen

En este Trabajo Final de Grado se realiza un estudio de la interacción entre un modelo de fármaco anticancerígeno, la curcumina, y modelos de membrana biológica constituidos por monocapas lipídicas en la interfase aire-agua. Este análisis se realiza utilizando la técnica de monocapas de Langmuir, donde se recogen las isotermas de presión superficial-área obtenidas al comprimir los filmes. En primer lugar y con el objetivo de aprender la técnica, se caracterizan las ampliamente estudiadas monocapas puras de colesterol (Chol), esfingomielina (Sph) y DDPC, obteniendo resultados que coinciden con la literatura. A continuación, se crean y analizan modelos de membrana celular sana y cancerígena usando monocapas mixtas de Chol: DDPC y Chol:Sph, concluyendo que la adición de colesterol a las monocapas puras condensa el sistema. Por último, diferentes cantidades de curcumina fueron añadidas en ambos modelos. El estudio de ciertos parámetros termodinámicos importantes, como son el exceso de energía libre ΔG_{exc} y el exceso de área superficial A_{exc} desvelaron que la curcumina penetra más en la membrana cancerígena, resultado que apoya el uso de este fármaco en estudios destinados a la creación de fármacos cancerígenos inteligentes.

Contents

1 Introduction

This Bachelor's final project has been developed in the Research Group on Fluids Physcics and Biocolloids of the Applied Physics Department at the University of Granada, more specifically within the framework of the project "Design of smart olive oil nanocapsules for oral administration: synthesis, physical-chemical characterization and in-vitro digestion, MAT2015-63644-C2-1-R". Researchers belonging to the Department of Applied Physics and the Anatomy and Embryology Department from the Medicine Faculty are involved in this multidisciplinary project, where the main goal is to develop an intelligent nanocarrier system of pancreas anticancer drug.

This treatment must be efficient and selectively attack cancer stem cells. In addition, one of the fundamental challenges of the project is the oral administration of the drug, therefore physical and chemical properties of the nanoparticles must guarantee the overcoming of all biological barriers the nanocarriers will face. A key of the process is to enter through cancer cell membranes and deliver the drug inside them, leaving the healthy ones inaltered. For this reason, this project aims to study the interaction between a model anticancer drug, curcumin, and both normal and cancer biological membrane models by using the Langmuir monolayer technique.

The systems analyzed in this research, known as monolayers, are monomolecular films that lay on the surface between two different media, in our case at the air-water interface. The main interest in using this technique lies in the fact that information on a molecular scale is acquired from a macroscopic analysis. In fact, first studies performed on the subject by Agnes Pockels (literally on her kitchen table, with a self-made balance prototype built with a pot and a button hanging on a scale) were directed to the determination of molecular sizes and for this reason these pioneering studies were object of interest of Lord Rayleigh [1].Their contributions helped Langmuir to lay laid the foundations for the study of these films.

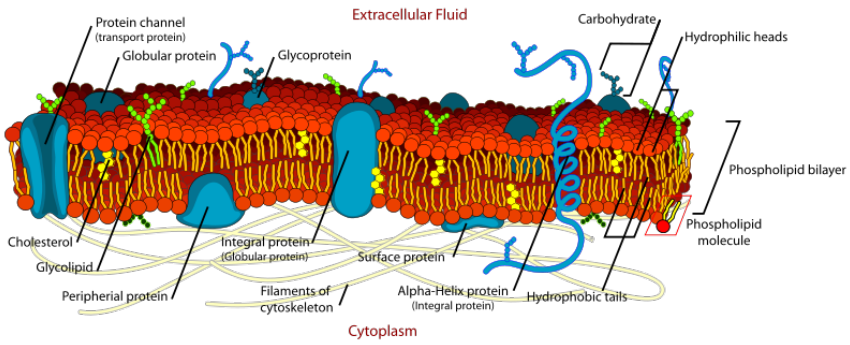

Figure 1: Biological cell membrane [2]

Langmuir monolayers at the air-water interface have been widely used to mimic cell membranes in attempts to determine the mechanisms involved in their interaction with bioactive molecules as this technique allows a fine control over the composition and packing of the membrane model [3]. Popular compounds used to prepare Langmuir monolayers are amphiphilic materials or surfactants, substances which possess a hydrophilic headgroup and a hydrophobic tail and locate spontaneously at the interface lowering the surface tension [4]. Lipids belong to this group, and their monolayers are in fact consid-

ered as a model for half a cell membrane [5, 6].

Numerous studies perform on membrane composition of normal versus cancer cells report a significant lower amount of cholesterol and the presence of unsaturated lipids in tumor cell membranes [7, 8]. These make cancer cells more fluid than normal cell and thus they do not interact with bioactive components in the same way. The molar ratio of cholesterol: phospholipids as well as lipid composition may differ depending on the kind of the cell and degree of malignancy, leading to the possibility of designing a huge amount of different artificial systems.

Throughout the current research work, a healthy cell membrane is modeled by a mixed monolayer of DPPC phospholipid and cholesterol (Chol) in a molar ratio Chol:DPPC=0.67 at the air-water interface, whereas the cancer analogous is composed of unsaturated sphyngomieline (Sph) and a lower proportion of Chol (Chol:Sph=0.25). Once both models have been completely described, curcumin is added to the systems and its effectiveness in the anticancer treatment is determined by studying its effect on the thermodynamic stability of both membrane models.

1.1 Objectives

The main objective of this Bachelor's final project is to study the interaction between a model anticancer drug, curcumin, and two biological membrane models: one corresponding to a healthy cell and other one to a cancer cell.

The specific objectives are:

- Interfacial characterization of two biological membrane models: healthy cell membrane model and cancer cell membrane model.
- Impact of addition of anticancer drug to the membrane models: effect of the curcumin, interactions between curcumin and membrane models

Moreover, this work pursues the following formative objectives:

- To develop a research work in experimental biophysics.
- To learn the use of current methodologies and design an experimental protocol to address an interfacial study of a biological material.
- To understand complex phenomena as those taking place in biological membranes.
- To study and understand current research in biophysics in order to adequately frame and discuss the experimental results obtained in the lab.

2 Theoretical background: thermodynamics of thin films on surfaces

Many fields related to physics and chemistry, such as Electromagnetism or Optics among others, contribute to the study of surface systems. In the current work, a thermodynamic approach is adopted together with certain numerical and statistical analysis given that the conclusions of the study are referred to molecules.

2.1 Monolayer formation and surfactants

For a substance to form a monolayer it must posses both a hydrophobic and hydrophilic nature. Amphiphilic molecules are made up of a polar group that is attracted by the water molecules and thus allows the spreading of the liquid over the surface, along with a non-polar portion which prevent the substance from sinking in the bulk and whose size must be large enough to counteract the interaction of the polar group.

When a drop of an insoluble liquid is placed on a clean water surface, three surface tensions act upon a infinitesimal element $\boldsymbol{\Delta l}$ of the drop line: one on the drop-air contact surface $\gamma_g \boldsymbol{\Delta l}$, one on the drop-water interface $\gamma_{ag} \boldsymbol{\Delta l}$ and last on the air-water interface $\gamma_a \boldsymbol{\Delta l}$, where the proportionality constant γ is known as *surface tension*. The first two tend to preserve the liquid contracted in a drop shape, whilst the latter spreads it over the surface. The final state of the liquid will depend on the balance of these two kind of forces, given by the so-called initial spread coefficient

$$S = \gamma_a - (\gamma_g + \gamma_{ag}) \tag{2.1}$$

If $S < 0$ the cohesive forces will predominate over the dispersive ones and a drop will form on the water surface, whereas it will spread in the case of $S > 0$. At equilibrium both fluids become saturated leading a null or negative spreading coefficient. The spreading drop can form a several molecules thick system, known as duplex film, or a monolayer at the air-water interface. Duplex films are metastable structures that always evolve to a drop or a monolayer.

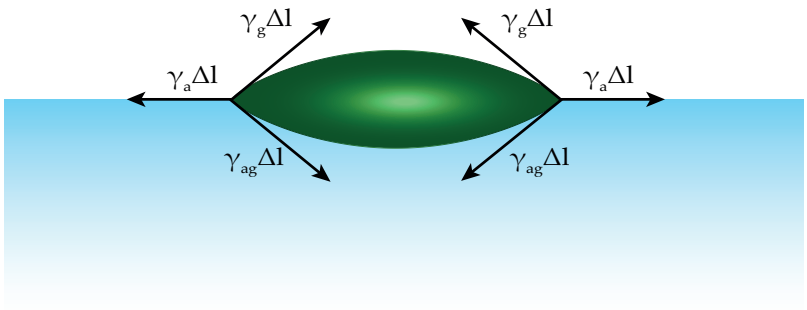

Figure 2: Surface tensions on a insoluble liquid drop deposited on a water surface.

The spreading coefficient is related with the change in Gibbs free energy by the first and second law of thermodynamics

$$dU = TdS - PdV + \sum_i \mu_i dN_i + dW \tag{2.2}$$

where the index i indicates the different substances. In this case, the differential work dW coincide with the superficial work γdA acting on an infinitesimal area element dA. Therefore, the Gibbs energy is given by

$$dG = -SdT + VdP + \sum_i \mu_i dN_i + \gamma dA \tag{2.3}$$

The Gibbs free energy G is usually more important than F because its natural variables, T and P, are constant in most applications. From 2.3 the surface tension follows:

$$\gamma = \left(\frac{\partial G}{\partial A}\right)_{T,P,N_i} \tag{2.4}$$

2.2 Basic concepts: surface pressure, molecular area and compressibility

The experimental data obtained from the compression of thin films at air-water interface allow to obtain a series of surface parameters, which provide broad information on the state of the monolayer, and thus on the structure and orientation of the constituent molecules. Some essential notions for the study of films are explained hereunder [9]:

- Surface pressure (π): surface pressure is the difference between the surface tension of a clean water surface γ_0 and that with a monolayer γ_m.

$$\pi = \gamma_0 - \gamma_m \tag{2.5}$$

- Mean molecular area (A) : ratio of the monolayer surface and its number of molecules. It is generally measured in $\mathring{A}^2/molec$.

- Compression modulus(C^{-1}): a useful parameter to study phase transitions in a isotherm is the monolayer compressibility. It can be obtained from $\pi - A$ data by means of the inverse of the surface elasticity C:

$$C^{-1} = -\left[\frac{1}{A}\left(\frac{dA}{d\pi}\right)_T\right]^{-1} \tag{2.6}$$

where A is area per molecule at a given surface pressure π. A large compression modulus indicates that the monolayer is more fluid and thus can be easily compressed. The compressibility along each phase of the film varies smoothly with the change in the mean molecular area, and, as will be explained in detail later, exhibits an abrupt change at transition.

Defining additional concepts related to those previously explained may be useful to study the properties of the films.

- Pressure and collapse area (π_c and A_c): define the point where molecules are forced to leave the air-water interface and form agglomerates above the monolayer, giving a threshold to the surface pressure. This value is detected by the abrupt drop of the superficial pressure at very small molecular areas values. Therefore, the collapse pressure is the highest pressure at which a monolayer can be compressed before becoming a non monomolecular film. More details are given in Section 2.3.

- Specific limit area (A_0): is obtained by extrapolating the linear part of the isotherm to zero surface pressure in the area of smaller areas per molecule. This parameter gives information about the orientation of the film molecules at a condensed state within the monolayer, which can be assumed to be roughly vertical. Consequently, A_0 is a good estimation of the molecule cross-section area.

2.3 Phases in surface systems

Monomolecular amphiphilic films show ordered phases similar to three-dimensional systems, that can be modified by changing variables such as surface pressure or temperature. These different states are determined by the interaction, stacking and orientation of the amphiphilic molecules, especially between their chains, and will be revealed to us through the shape of the $\pi - A$ isotherms (Fig. 3). Generally, a film display four main states: gaseous, expanded, condensed and collapsed . Nonetheless, the notation differs depending on the author [9].

2.3.1 Gaseous films

The simplest state showed by a monolayer, where the forces between surfactant chains are negligible due to the large molecular separation and therefore molecules are lying almost horizontally on the surface. The average area per molecule on the surface is much larger than the size of the molecule and the measured surface pressure is very low . The kinetic analysis of this state is analogous to the kinetic theory of three-dimensional gases, where the molecules move with a translational kinetic energy equal to $1/2kT$ per degree of freedom, therefore a bidimensional gas obeys the equation:

$$\pi A = kT \tag{2.7}$$

This expression is only completely valid at extremely high areas and low surface pressures given that the linearity between πA and π or A is broken when the film is compressed as a result of the non-zero size of the molecules. Consequently, corrections have been made to the equation, introducing an adjustable parameterA_0 asociated with the observed molecule area in condensed films:

$$\pi(A - A_0) = kT \tag{2.8}$$

In addition, when the monolayer is spreaded an the air-water interface, negative deviations are found in the case of electrically neutral monolayers due to the arising of attractive forces between the film molecules analogous to Van der Waals forces in gases [1]. which would require the introduction of another correction term:

$$\pi(A - A_0) = qkT \tag{2.9}$$

where q is lower than 1, generally 0.7.

2.3.2 Expanded films

The expanded monolayers, also known as liquid-expanded state (LE), have an intermediate molecular area between gaseous and condensed films due to an intermediate packaging of the molecules. The hydrophobic fraction of the particles are randomly distributed and only the polar functional groups are in contact with the subphase,. The $\pi - A$ diagrams of a expanded monolayer show isotherms with a greater slope than in the gaseous case and a mean molecular area which is around three times the cross section of the molecule[9].

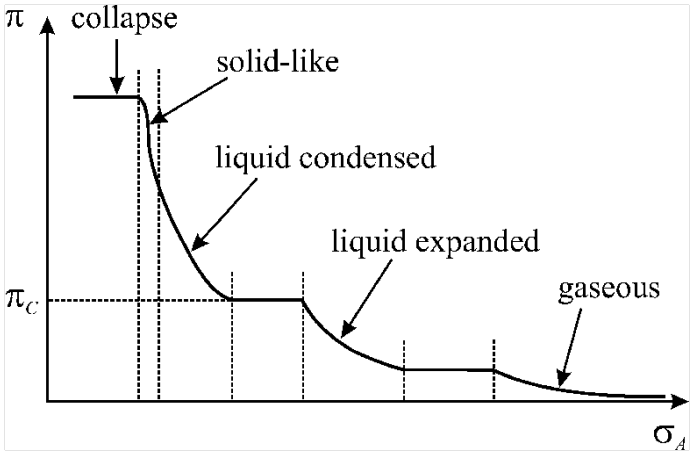

Figure 3: Schematic graph of a $\pi - A$ isotherm showing the different phases and phase transitions which can occur in a monolayer. [2]

In his quantitative interpretation, Langmuir considers that the film behaves like a pure hydrocarbon, thus shows a surface tension characteristic of a normal liquid. Hence, a corrective coefficient π_0 is added to Eq. 2.8 to take into account the surface pressure variation due to the extension of the hydrocarbon part of the molecules on the water surface:

$$(\pi - \pi_0)(A - A_0) = kT \tag{2.10}$$

2.3.3 Condensed films

Under further compression, molecules begin to be closed-packed and the film reaches the condensed or liquid condensed state (LC). Only when attractive chain-chain forces are of greater importance than repulsive interactions an insoluble monolayer can exist at low surface pressures, so molecules must interact closely.

Electron diffraction experiments performed on monolayers transferred to solids show that the chains are oriented almost vertically to the surface, therefore $\pi - A$ isotherms show small variations with the length of the carbon chain and the area occupied by a molecule is substantially independent of the number of carbon atoms of the saturated chain. In addition, the graphs are practically perpendicular to the abscissa axis, indicating a low compressibility of these monolayers. In the higher pressure region of these diagrams, just before collapsing, the curve shows a high slope and the smallest molecular area corresponding to the maximum packing configuration approximates the true cross section of the molecule.

Small variations in the behavior of different monolayers have led to several authors to postulate different surface phases within the category of condensed films . However, considering them does not add any relevant information to our analysis, so all these states will be classified as LC states.

Several models of state equations can be used to describe the behavior of a monolayer including further interactions. The most general is the widely known virial expansion:

$$\frac{\pi A}{kT} = b_0 + b_1\pi + b_2\pi^2 + ... \tag{2.11}$$

where it is possible to obtain information on the intermolecular forces from the virial coefficients b_i.

Another model is the approach proposed by Birdi et al. [10]. As mentioned above, for an ideal interfacial monolayer the considered equation of state is Eq. 2.8 where only the movement of the particles due to temperature contribute to the surface pressure. It is convenient to label this kinetic contribution as π_k from now on to distinguish it from other corrections. Due to the presence of interactions, a difference π_i between π_k and the measured surface pressure π has to be considered. Including the previously defined occupied molecular area correction term A_0 and a corrective factor ϕ_h due to the hydration of the molecules [11] the interaction term becomes:

$$\pi_i = \pi - \frac{kT}{A - \phi_h A_0} \tag{2.12}$$

If $\pi_i > 0$ the dominant interaction is repulsive, usually electrostatic, whereas if $\pi_i < 0$ the net force is attractive, mainly Van der Waals type interaction. Consequently, 2.12 can be written as:

$$\pi = \frac{kT}{A - \phi_h A_0} + \pi_{vdw} + \pi_{elec} \tag{2.13}$$

Neglecting π_{elec} for low charged molecules and assuming hexagonal packaging [10] leads to the final equation of state:

$$\pi = \frac{kT}{A - \phi_h A_0} + c_1 + \frac{c_2}{A^{2.5}} \tag{2.14}$$

where c_1 and c_2 are constant proportional to the van der Waals dispersion forces.

Other models have been obtained considering different kinds of interactions, allowing to describe a wide range of monolayer of different substances. As an example, two models proposed by Fainerman et al. [12] (Eq. 2.15) and Brockman et al. [13] (Eq. 2.16) which were initially considered candidates for state equations are shown below:

$$\pi = \frac{RT(A/A_c)^2 e^{-2\triangle\pi\epsilon A_1/RT}}{A - \omega_1\left\{1 + \epsilon\left[(A/A_c)^2 e^{-2\triangle\pi\epsilon A_1/RT} - 1\right]\right\}} - B_\Sigma \tag{2.15}$$

$$\pi = \frac{qkT}{A_1} ln\left[\left(\frac{1}{f_1}\right)\left(1 + \frac{A_1}{A - A_0}\right)\right] \tag{2.16}$$

with A_c the collapse area, A_1 the area of an interfacial water molecule, f_1 the activity coefficient of the water, and q a parameter included to allow for higher order terms involving the activity coefficient.

2.3.4 Collapsed films

At smaller values of surface area, the phenomenon "collapse" occurs and the compressibility of the monolayer approaches infinity. The beginning of the collapse depends on facts

such as the previous history of the film and the compression speed. During the collapse, the monomolecular layers are placed one on top of the other, which causes the formation of disordered multilayers and the rupture of the monolayer.

Several criterion can be established in order to determine the stability conditions of the collapse[1]. Some examples of acceptable collapse indicators are the sudden pressure drop if the area is constant over time, the reduction in the area of the film over time under constant pressure or the maximum pressure detected at a certain compression speed, being the second one the most widespread among authors.

2.4 Phase transitions

Like other thermodynamic systems, monolayers exhibit phase transitions between states. Through this section the different kinds are analyzed. Two types of transitions can be considered: main and secondary transitions. However, in our study only the main ones are relevant.

At very low surfaces, a first order main transition from the LE or LC state to the gaseous state takes place. It is characterized by a constant vapor pressure and in most cases this transition is not measured with the Langmuir balance technique. A more obvious main transition is observed between LE and LC states characterized by a practically constant surface pressure value. The order of this phase transition has been discussed by different authors, but some of them have presented experimental evidence of a first-order transition [14]. Therefore, $\pi - A$ isotherm must exhibit an horizontal region in the coexistence region, as shown in Fig. 3, and the compression modulus an inflection point.

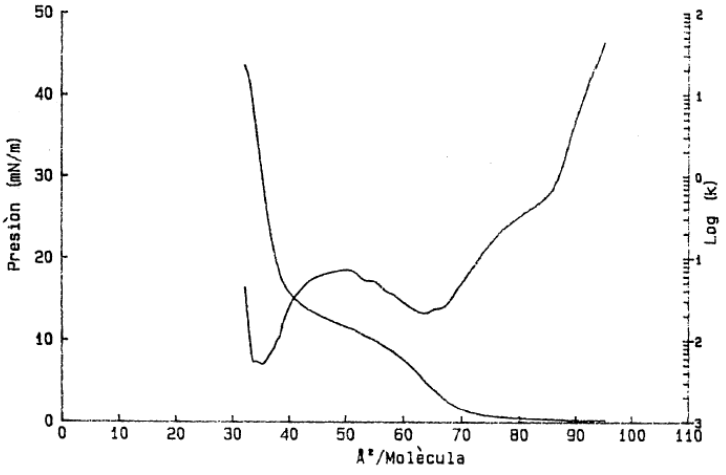

Figure 4: Experimental isotherm (left vertical axis) and compression modulus (right vertical axis) versus mean molecular area showing a phase transition [9].

In practice, a slope appears in the transition region due to intrinsic properties of the molecules [9] which hinders its analysis. Albrecht et al. [14] proposed to study the shape of the $C^{-1} - \pi$ or $C^{-1} - A$ curves to address this problem. Since the slope of the $\pi - A$ isotherm is almost null at coexistence, C^{-1} will not be infinite as in the ideal case but will show a maximum at the transition region as shown in Fig. 4. Other authors [15] determined exact starting and ending transition points by comparing the first three derivatives.

2.5 Mixed-films

In studies of monolayers made up of multiple components, the type of film formed may vary depending on the molecular interactions among the constituents. Structurally similar materials cause the characteristics of the monolayer to lie between that formed by each separately due to the homogeneous distribution of the components throughout the film and the lack of interaction amongst them. If dissimilar substances are mixed they can undergo interactions which different effects in the observed isotherms. For strong interacting materials (inmiscible substances), the layer becomes more condensed since the forces arising from those interactions can induce some molecules to partially penetrate into the liquid film or locate on top of the others. If the substances are different enough and no specific interactions occur, increasing the surface pressure may yield the total expulsion of one component from the surface. In the absence of the aforementioned effects, a heterogeneous film may be formed, with well defined regions of different films, resembling a two-dimensional emulsion or dispersion [16].

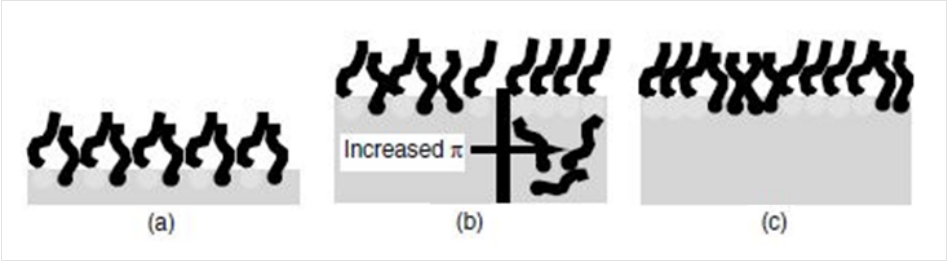

Figure 5: Possible structures in mixed molecular films. (a) Ideal mixed film, (b) inmiscible components and (c) heterogeneous film [16].

2.5.1 Thermodynamics of Mixture

The research reflected in this report involves the study of mixed-monolayers

The properties displayed on the π-A isotherm of mixed-films mainly depend on the sort of interaction existing between the molecules of the different components, what is reflected in their miscibility. Miscibility of the monolayer substances can be analyzed under the formalism of the Thermodynamics of Mixture , where the variations in the main thermodynamic functions during the compression process are evaluated in terms of surface pressure . For a generic quantity Z, with the variation in the mixing process $\triangle Z$, the excess mixture magnitude Z_{exc} can be defined [17]:

$$Z_{exc} = \triangle Z - \triangle Z_{id} \tag{2.17}$$

where $\triangle Z_{id}$ denotes a hypothetical ideal mixture of the components. In this study, we will focus on the comparison of the deviation between the experimental mean molecular areas of the ternary film A_{123} and their ideal values A_{id} when a third component is added to a binary monolayer. In a mixture with a component concentration χ_3, expressed as mole fraction, A_{id} results from the additivity rule:

$$A_{id} = A_3\chi_3 + A_{12}\left(\chi_1 + \chi_2\right) \tag{2.18}$$

wherein A_3 is the area per molecule of the third in its pure film, A_{12} is the mean area per molecule in the binary monolayer, and χ_1 and χ_2 are the mole fractions of the two components in the mixed film. Therefore, the excess area is given by:

$$A_{exc} = A_{123} - A_{id} = A_{123} - A_{12}\,(\chi_1 + \chi_2) - A_3\chi_3 \tag{2.19}$$

Inmiscible or ideally miscible but not interacting components generate a straight line at the origin in the mean molecular area excess versus composition plots given that all the different molecules are placed right on the surface and, therefore, the area per molecule is expected to be an average of the molecular areas of the different substances. The deviations from linearity suggest a non ideal behavior and miscibility of the monolayer components. Positive values of A_{exc} indicate that molecules in the mixed film occupy a larger area than in the ideal case due to the presence of repulsive interactions between the components. Negative deviations from ideality, by contrast, suggest attractive interactions among the molecules and the formation of bidimensional clusters. However, these diagnoses must be corroborated by energy analysis [18].

Consequently, in order to evaluate the interactions between curcumin and a mixed monolayer, the excess free energy of mixture has been calculated:

$$\Delta G_{exc} = N \int_0^{\pi} (A_{123} - A_{12}\,(\chi_1 + \chi_2) - A_3\chi_3) d\pi \tag{2.20}$$

Negative values of ΔG_{exc} are the sign of strong interactions between the three components whereas a positive ΔG_{exc}reveals repulsive interactions between monolayer components. When $\Delta G_{exc} = 0$, the mixing is ideal [18, 19].

3 Materials and methodology

3.1 Lipids in biological membrane models: DPPC, Sph y Chol

In the experiments, the cell membranes have been modeled with Langmuir films composed of the following human membrane lipids.

- Cholesterol (Chol)

Cholesterol is the principal sterol (organic compound with four rings in its molecular configuration) of all vertebrates, mainly distributed in body tissues, especially the brain and spinal cord, fats and animal oils. It is an important component of cell membranes, providing stability due to its ring-like structure, and a precursor for the biosynthesis of biological molecules such as vitamin D or bile acid. In the body, cholesterol can be found in either the free form or as an ester with a single fatty acid (a carboxyl group R-COOH with a chain of 10-20 carbons in length) covalently attached to a hydroxyl group R-OH at position 3 of the cholesterol ring (Fig. 6). The molecular weight of the used cholesterol was 386.65 g/mol [20].

- Dipalmitoylphosphatidylcholine (DPPC)

Dipalmitoylphosphatidylcholine is a synthetic phospholipid widely used in monolayers and lipid bilayers to study biological membranes. Like other phospholipids, DPPC structure consist on a polar head with a phosphate group PO_3^{-4} attached to fatty acid tails, in this case two saturated carbon chains, as shown in Fig. 6. It is the major constituent of many pulmonary surfactants, substances that reduce surface tension of alveoli by adsorbing to their air-water interface, what prevents fluid accumulation and keeps airways dry [4]. In addition, having a negative charge on the phosphate group and a positive charge on the quaternary ammonium group gives DPPC a zwitterionic nature (a "zwitterion" or dipoar ion is a globally neutral molecule formed by functional groups, of which at least two are electrically charged with opposite sign [21]). DPPC molecular weight is reported to be 734.00 g/mol.

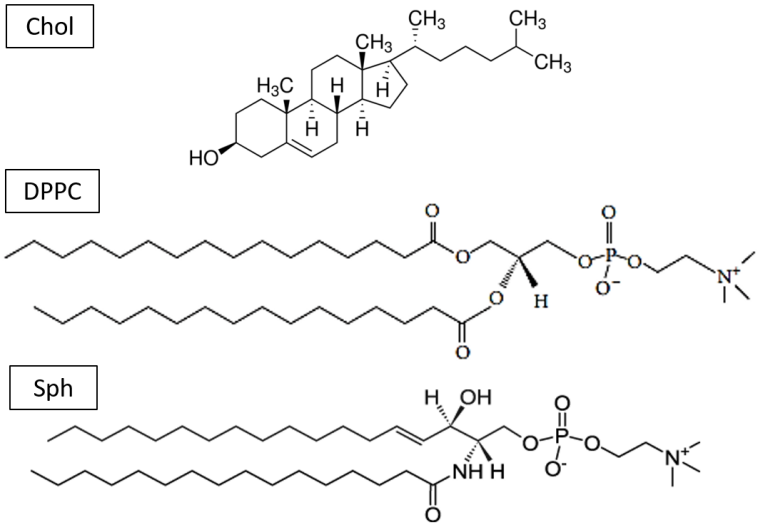

Figure 6: Molecular structure of the different lipids [22, 23].

- Sphingomyelin (Sph)

Sphingomyelin is a type of sphingolipid found in animal cell membranes, especially in the myelin layer around nerve cell axons. Like all sphingolipids, Sph has a so called ceramide core: an hydroxyl and amino group bonded to an unsaturated hydrocarbon chain and a fatty acid, as shown in Fig. 6. This composition yields to a three-dimensional structure with no net charge on the head groups [20]. In humans, sphingomyelin represents the 85% of all sphingolipids and plasma membrane of cells is highly enriched in this component.

Different length of carbon chains can be found in sphingomyelin structure and generally commercial products contain a non specified mixture of molecules constituted by 30 to 40 carbons atoms approximately. The diverse interactions arising between them alter the resulting isotherm outline depending on the content of each kind of Sph [24]. However, only this factor should be taken into account when comparing with the bibliography, since the same mixture was used in all the Sph solution made within this project. In calculations, a molecular weight of 703.00 g/mol was considered.

All the monolayer components were purchased from $Sigma - Aldrich\ Inc^{®}$, stored at 4 °C and used without further purification.

The normal cell membrane was prepared by mixing of cholesterol and DPPC in a molar proportion of Chol:DPPC=0.67 whereas the tumor cell model membrane was composed of sphingomyelin and a lower concentration of cholesterol: Chol:Sph=0.25. The choice is based on Hac-Wydro et al. [7] and Inbar et al. [8] works , where a significant difference in the amount of cholesterol was found between healthy and tumor cell membranes. Malignant transformations are associated with changes in the dynamic properties of cellular membrane, causing the cancer cell membrane to be more fluid. This results in considerable reductions on the cholesterol concentration present in the tumor cell with respect to the healthy analogous [3]. In addition, DPPC was replaced with Sph since it is an unsaturated lipid, thereby films constituted mainly by this lipid are less cohesive and less condensed.

3.2 Anticancer drug model: Curcumin (Cur)

Curcumin is a yellow-orange compound obtained from the powdered root of the turmeric plant Curcuma longa, a member of the Zingiberaceae family [25]. Cur has been usually used as a natural spice, mainly in curry, for a long time. Recently, it is being used as food preservative, coloring agent and dietary. Several studies have reported benefits on health of curcumin, such as anti-inflammatory, antioxidant, antibiotic or antiviral properties due to its inhibitory effects on metabolic enzymes[20]. Anticancer properties of this compound involve the inhibition of the growth of the cancer cells by altering their gene expression and the cell cycle [26]. Curcumin molecular weight is 368.39 g/mol and is considered to be a natural acid polyphenolic since its molecular structure, which is represented in Fig. 7, is mainly formed by two phenol groups C_6H_5OH

Curcumin was purchased from $Sigma - Aldrich, Inc^{®}$, stored at room temperature and used without further purification.

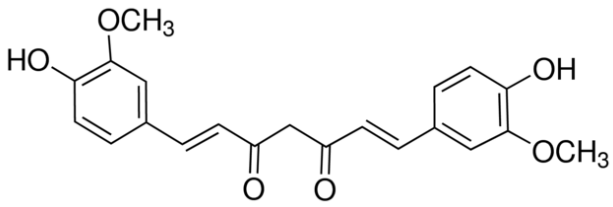

Figure 7: Curcumin molecular structure [23].

3.3 Preparation of the solutions

The different substances where deposited on the surface in solution form. The solvent for solutions involving only DPPC and cholesterol was high purity chloroform from Scharlab S.L ($CHCl_3$ stabilized with ethanol, $Multisolvent^{®}$ HPLC grade). Given the difficulty of solving Sph and Curc in a polar substance as the $CHCl_3$, a methanol-chloroform mix in a 1:4 ratio was used for these substances. The solutions were prepared using a high precision scale , a $Hamilton^{®}$ 700 series fixed needle syringe and a 5 ml $Nahita^{®}$ class A volumetric flask, and stored in small glass containers with screw tap, some of them holding a sponge to introduce the syringe. All tools and recipients were thoroughly washed before each usage with Micro 90 soap, tap water, isopropanol, distilled and ultrapure wa-

ter, in this sequence.

3.4 Subphases

Double distilled water (Millipore Milli-Q Reagent Water System) was utilized as a subphase for some monolayers as well as for cleaning purposes and to prepare the buffer and the solutions. Conductivity of the water obtained after this process was always lower that 1 $\mu S/cm$ and its pH was 6-6.5.

Most solutions were spread on a phosphate buffer at pH 7 (conductivity of 400 $\mu S/cm$). In order to prepare 1 l of this solution 1.56 mg of sodium dihydrogen phosphate monohydrate, reagent grade, ACS (NaH_2PO_4, purchased from Scharlab S.L, CAS: 10049-21-5, and stored at room temperature) was dissolved in 500 ml of double-distilled water in a 600 ml beaker with the help of a magnetic stirrer. The pH of the resulting substance was then adjusted with $NaOH$ and HCl to obtain a pH 7 solution. Finally, the solution was transferred to a 1 l volumetric flask, was filled to the mark with double-distilled water and stored at in a glass bottle. The subphase temperature was fixed to 23 °C by a circulating water system connected to a thermostat.

3.5 Langmuir film balance

The experimental device used to obtain all the surface pressure-area isotherms was the KSV Minitrough from KSV Instruments, a commercial version of a Langmuir-film balance. The apparatus consists of three main elements (see Fig. 8):

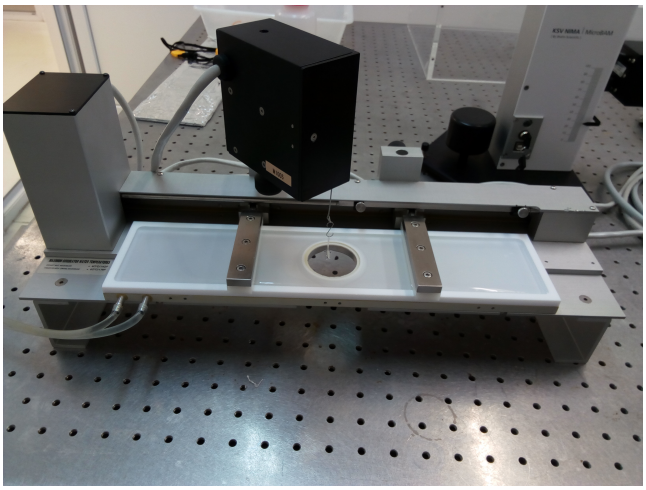

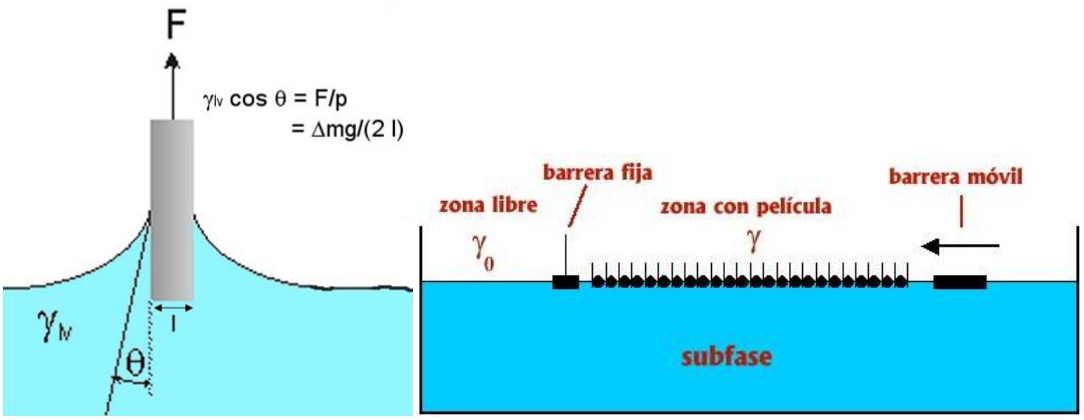

Figure 8: Langmuir film balance and schematic overview of its operation. Picture courtesy of the Applied Physics Department at the University of Granada.

- Through: the subphase and monolayer are deposited into a teflonized aluminum tray with a total area of 27375 cm^2(365x75x5 mm) connected to a temperature regulation system. The coating of the through gives the surface a hydrophobic nature that allows its filling above its geometric possibilities without breaking the film, preventing the passage of the film deposited under the fixed barrier to the free zone thereof. In addition, it allows to clean and empty the tray easily an is very resistant to most organic components.

- Barriers: the film was symmetrically compressed by means of two moving barriers drived by a servo DC motor. As with the tray, they are teflon-covered and, moreover, they can be extracted facilitating the cleaning labors. Four metallic blocks placed at the end and center of the barriers rail limit the area of compression to a range between 237.75 cm^2 and 43.07 cm^2.

- Surface pressure measuring system: surface pressure was measured using a Wilhelmy plate made of filter paper, recorded by the electrobalance to which the device is connected and sent to the computer . Surface pressure was measured using the Wilhelmy method,which is the most commonly used to measure surface pressure of plane and fluid interfaces. A filter paper was partially immersed in the water substrate. The forces acting on the paper are its weight P, the surface tension acting downward, and Archimedes force A. The net downward force is:

$$F = P + 2\,\gamma_{water}\,l\,cos\theta - A \tag{3.1}$$

where l is the length of the shorter side of the paper and θ is the contact angle of the liquid. If the plate is completely wetted the contact angle $\theta = 0$ so $cos\theta = 1$. When the composition of the interface varies, P and A stay constant but surface tension changes to γ_{sol}. This change is compared to the values of surface tension of water:

$$\Delta F = 2l(\gamma_{sol} - \gamma_{water}) = -2l\pi \tag{3.2}$$

and the surface pressure is obtained using:

$$\pi = -\Delta F/2l \tag{3.3}$$

The setup is placed on an anti-vibration table to avoid any disturbance in a basement in extreme cleanliness conditions and with a proper ventilation system. All this components were interfaced to a software written in C++ for WindowsTM 2000 and XP (KSV LB software) allows the user to control the setup as well as visualize, process and store the data [27].

3.5.1 Cleaning and calibration

The cleaning of the device was a fundamental operation to undergo before each experience. Any kind of impurity had an extraordinary impact on the results obtained when handling surfaces for study, thereby it was highly important to work in conditions of extreme cleanliness when performing the experiments. All the steps of the cleaning process had to be followed meticulously to avoid contamination. First, the through and the barriers were rubbed with a lint-free wiper impregnated with pure isopropanol. Then, the through was filled several times with double distilled water and emptied using a rubber tube connected to a laboratory vacuum cleaner.

Before placing the surfactant the surface was vacuumed and the presence of impurities was tested closing the barriers and checking that the surface tension did not rise above 0.5 mN/m. The aspirate of the surface or, in the worst case, the complete cleaning process had to be repeated if this condition was not met. The syringes employed in solution spreading had to be flushed with chloroform before and after each use. At the end of the experiment, the surface was first aspirated maintaining the barriers closed in order to remove the largest amount of surfactant possible, the through was emptied and the cleaning process was repeated.

Calibration of the pressure recorder was also an important task. Prior to any experiment, just after the opening of the software, surface pressure was set to zero and a small metal ring was suspended, together with the filter paper, from the balance filament. Values of surface pressure under those conditions within the range 250 ± 1 mg guarantee a proper calibration. In case of disagreement, the surface pressure with and without the ring were compared using the software to restore the pressure reference value.

3.5.2 Monolayer formation procedure

Once the cleaning process was finished, the through was filled with buffer and the solution was carefully spread on its surface in the form of small drops with the help of a syringe. Before compression, the monolayers were left for 10 min, a time estimated to be sufficient to let the solvent of the different solutions to evaporate with the purpose of reaching equilibrium without contaminating the film before conducting the experiments. After that time, barriers began to close automatically until the minimum area is reached, and the balance software started to record all the data.

The temperature was fixed to 23 °C with the help of the thermostat . Although the films extend when increasing the temperature due to the fact that thermal excitation reduce the van der Waals attractive forces [17], this effect is not significative so can be neglected in the present study, therefore all the experiments had been conducted under the same temperature conditions. [11].

In most solutions, a concentration of $0.5\,mg/ml$ was used and $50\,\mu l$ of volume was

delivered, so in Section 4 it will be considered that these are the quantities used unless otherwise indicated in specific circumstances where it was necessary to change them to obtain a correct result.

3.6 Experimental errors

There are several errors that may be considered in each experiment. The accuracy in the surface pressure measurements were 4 μN according to the device specifications [27]. Nevertheless, for each solution a minimum of two different isotherms were recorded in separate days to ensure the reproducibility of the results. Hence, the final surface pressure considered in the isotherm analysis was the average between the values of all the equivalent monolayers, taking the resulting standard deviation as the error.

A large amount of different solutions where used in the experiments, therefore the most unfavorable error was considered in all cases. One-component solutions were prepared weighting masses lower than 10 mg with the scale ($\pm$0.01 mg) and using a 5.000 $\pm$ 0.025 ml flask, yielding an upper error threshold of 0.011 mg/ml. Mixtures needs to take into account the previous calculated uncertainty, the accuracy of the syringes used to measure small volumes when mixing (no higher than 0.50 $\pm$ 0.01 ml) and the flask precision. The concentration of the final solution is:

$$\rho = \frac{1}{V_{flask}} \sum_i V_i \rho_i \tag{3.4}$$

wherein V_i and ρ_i are the volume and concentration of each solution. All the mixtures were prepared with less than three substances, thus the highest uncertainty obtained for the solution concentration is 0.015 mg/ml.

The uncertainty in the mean molecular area was calculated by error propagation of the following formula:

$$Mma = \frac{A}{no.\,molecules} = \frac{A\,Mw}{V\,\rho\,N_A} \tag{3.5}$$

where A is the compression area, Mw the molecular weight, V the deposited solution volume, ρ its mass-volume concentration and N_A the Avogadro constant. The error considered in the delivered volume was $\pm$0.5 μl when the 25 μl syringe was employed and $\pm$1 μl for the 50 μl and 100 μl syringes, and $\pm$0.01 g/mol for the molecular weight. The device was able to measure the compression area with an accuracy of 1% [27].

4 Results and Discussion

In the following, the results of all the experiments that have been carried out along with their detailed analysis are presented. The followed experimental process had been already explained in Section 3.5.2.

4.1 Preliminary experiments: Langmuir through usage and control

In order to make initial contact with the experimental device and optimize the parameters to obtain the upcoming monolayers the surface pressure (π)–area (A) isotherm was

recorded for pure DPPC, Sph and Chol on Milli-Q water substrate, all well studied and with numerous references in the bibliography [9, 15]. The concentration and volume of the spread substance played an important role in the process since they determine the number of molecules of the film. If few molecules were placed at the interface the distance between them when compressing was insufficient to obtain a liquid condensate state due to the weak molecular interaction, whereas large quantities yielded to initially condensated films which tended to penetrate in the subphase and collapse. Consequently, several solution concentrations were tested for each substance in order to determine the spreading amount.

The compression rate was also varied as the applied model assumes the system to be at equilibrium and hence, to compress at a sufficiently low rate was requisite to allow the relaxation of the monolayer, but also it was also desirable to optimize the experimentation time. For this reason, the barrier compression rate was varied in a range of 5mm/min and 50 mm/min, detecting that high compression rates cause more abrupt phase transitions since molecules have no time to reorient their chain above the surface and thus the interaction between neighbors is stronger. Therefore, the optimal rate was the highest speed at which isotherm outlines did not change when further decreasing the compression rate. In view of these results, 10 mm/min was considered to be a proper barrier speed to perform the forthcoming experiments.

4.2 Pure monolayers

A spreading of each pure film with the optimized parameters along with their compression modulus are displayed in Fig. 9.

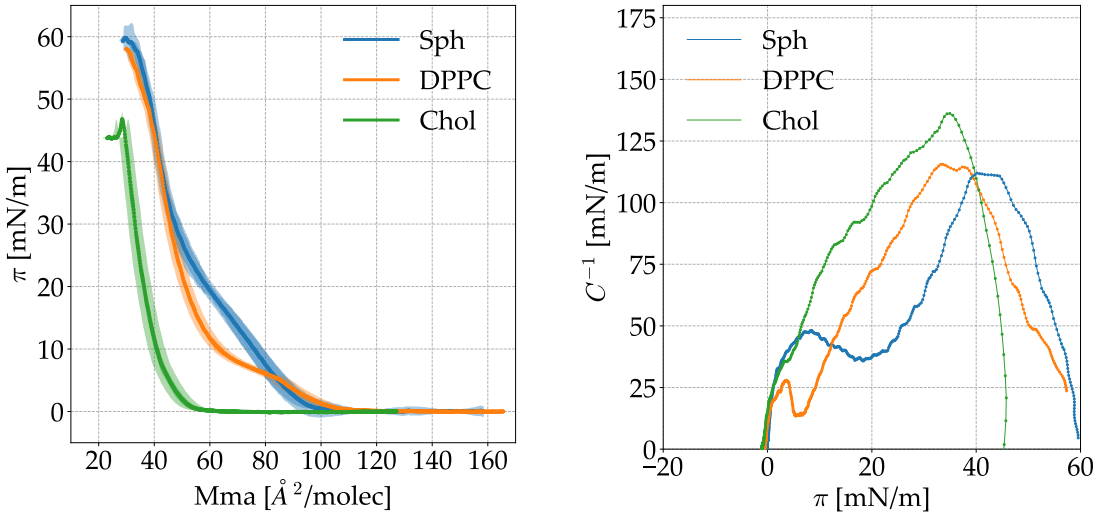

Figure 9: On the left, surface pressure π versus mean molecular area Mma isotherms for pure Sph, DPPC and Chol. On the right, compression modulus C^{-1} as a function of the surface pressure. Shaded areas represent data uncertainty. Errors in C^{-1} are not shown for clarity.

In this case, concentrations of 0.5 mg/ml where used, delivering 35 μl of Sph and

50 μl of Chol and DPPC. The specific limit area for each system has been calculated using Python by elongating the liquid condensed phase of the monolayer towards the horizontal axis in order to check the validity of the results. Values around 57.9 $\AA^2$, 53.5 $\AA^2$ and 35.4 $\AA^2$ were obtained for the Sph, DDPC and Chol film respectively[1]. Table 1 contains this values together with other parameters of interest. The shape of the three monolayers together with the values of the molecular areas are in agreement with literature works [9, 15, 28].

The shape of the (π-A) isotherm for pure cholesterol suggests the existence of a packing of vertically oriented molecules given their higher rigidity due to the presence of a tetracyclic ring in its structure, so that cholesterol monolayers can be considered to be condensed. Hence, the isotherm is practically perpendicular to the area axis for surface pressures within the whole compression range. Furthermore, molecular models show that both the geometry of the whole cholesterol molecule and the location of the hydroxyl group favor the formation of strong, stable monomolecular film for this lipid [29]. As a consequence, a low limiting specific area per molecule and collapse pressure are observed in Table 1 . The most noticeable property of the monolayer is, however, the low compressibility (high rigidity) of the film (see Table 1)[2], which determines the condensed film behavior and justifies the proposed vertical packing. Indeed, it shows the highest values of the compression modulus and only a global maximum corresponding to the collapse, evidencing the lack of LE/LC transition.

The (π-A) isotherm for pure DPPC distinctly shows a phase transition between LE and LC states, represented by a local maximum in the compresibility modulus at low pressures (see Table 1) in agreement with literature[17]. The more extended character of DPPC film as compared with cholesterol monolayer is demonstrated by the lower values observed for the compressibility modulus and the higher limiting specific area. This means that during the first steps of compression the extended film can be considered to be a liquid phase of low thickness, in which the molecules show some inclination to the surface, where the polar groups are in contact with the subphase. The LE/LC transition can be explained by a molecular reorganization by virtue of which the molecules are strongly packed and perpendicular to the surface when the transition is finished. The transition region does not correspond to a plane portion of the isotherm. Albrecht et al. [14] showed that the finite slope was an intrinsic property of the monolayer, originating from additional surface pressure due to the repulsive electrostatic interaction between the electric dipoles at the polar groups of the molecules. Other authors [30] confirmed that DPPC molecules have "zwitterionic" character in a middle pH range, and it is well known that an arrangement of parallel dipoles orientated perpendicularly to the surface can provoke repulsive interactions, which would explain the high values of the specific molecular area obtained.

[1] Errors are not shown as they are approximate values obtained by extrapolation

[2] Errors are not shown because these values are obtained by extrapolation.

Isotherm	A_0 [$\AA^2$]	π_c	C_{max}^{-1}
Sph	72.08	60.21	65.47
DPPC	71.48	58.10	108.10
Chol	48.42	46.44	118.52

Table 1: Specific limit area A_0, collapse pressure π_c and compression modulus C_{cell}^{-1} at cell membrane lateral pressure for pure Sph, DPPC and Chol.

In the case of the Sph, the film is more extended when compared with Chol and DPPC monolayers. This behavior is due to the different structure of the hydrocarbon chains, asymmetric and with the presence of a double bound, that causes the emergence of stronger repulsive interactions among them. For this reason, the LE/LC phase transition is less pronounced than the exhibited by the DPPC film, generating a lower compressibility modulus with smoother extreme which appear at higher surface pressures (see Table 1). However, both DPPC and Sph present a very similar specific limit area since the transversal area of both molecules is similar.

4.3 Healthy cells model membrane (Chol:DPPC=0.67)

The Chol:DPPC mixed monolayers isotherm modeling the normal cell is shown in Fig. 10 together with the pure constituents and compression modulus for a better analysis.

The (π-A) isotherm corresponding to the Chol:DPPC mixed monolayer shows a somewhat intermediate behaviour compared with that shown by pure components. When cholesterol is added to DPPC, the average cross sectional area per molecule of it isotherm decreases and therefore the isotherm of mixed monolayer appears between the isotherms of the pure components. As it was explained in Section 4.2, cholesterol forms at the air-water interface highly condensed monolayers, which reflects in a low area per molecule, high values of compression modulus and very steep course of the isotherm. When mixing with the Chol, the compression modulus shifts towards higher values (see Table 2) even exceeding the values found for pure cholesterol. Then, the presence of cholesterol in a mixed monolayer provoke an effect of condensation on the film of the other lipid.

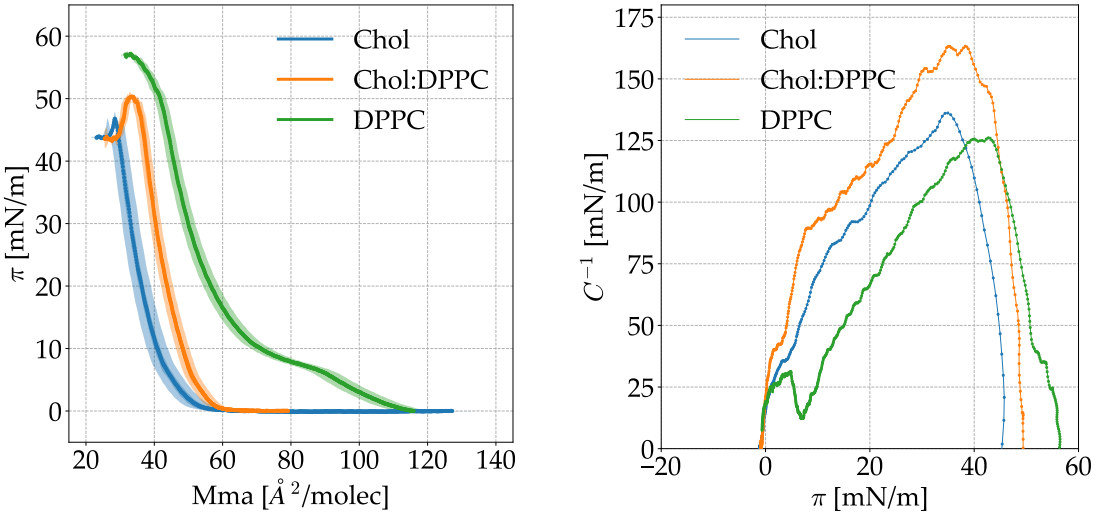

Figure 10: Surface pressure π versus mean molecular area *Mma* isotherms and compression modulus C^{-1} as a function of the surface pressure for pure DPPC and Chol, and mixed Chol:DPPC=0.67 monolayers.

In addition, the maximum of C^{-1} at low surface pressure regions in the pure DPPC vanish, what reflects the absence of LE/LC transition in the mixed layer. Chol:DPPC isotherm thus adopts to some extent the shape of the cholesterol isotherm. This is known as the "condensing effect" of cholesterol on DPPC, and has been interpreted [29] on the basis of either molecular packing or specific interactions between the compounds forming the mixed monolayer. Values for the different parameters are presented in Table 2.

4.4 Tumor cells model membrane (Chol:Sph=0.25)

Fig. 11 presents the (π-A) isotherms of Chol:Sph mixed monolayers modeling a tumor cell membrane together with the pure constituents. The Chol:Sph model mixed monolayer also presents a somewhat intermediate behavior compared with the shown by pure lipids, Chol and Sph. In this case, the condensing effect of cholesterol on Sph is less pronounced since, as discussed earlier, the pure Sph film is rather extended and the proportion of Chol in this membrane model is low. The maximum of the compressibility modulus, which correspond to the pressure of the LC state, shifts towards higher values (see Table 2). Note that the condensation of the film causes the transition LE/LC to be visible in the Chol:Sph isotherm, i.e. the compression modulus displays a sharp maximum and later minimum, which is not noticeable in the looser Sph film.

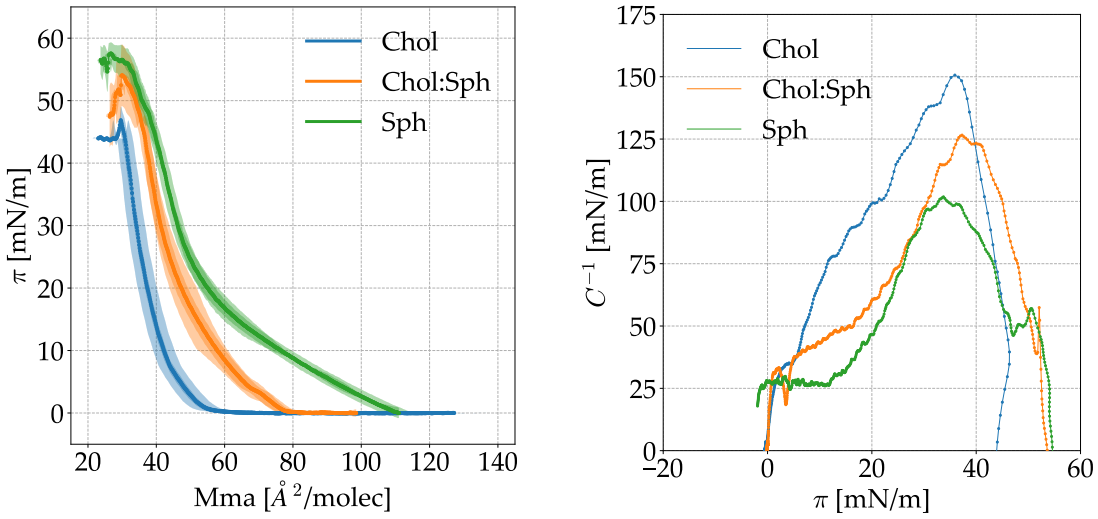

Figure 11: Surface pressure π versus mean molecular area *Mma* isotherms and compression modulus C^{-1} versus surface pressure for pure Sph and Chol, and mixed Chol:Sph=0.25 monolayers.

4.5 Curcumin anticancer drug interfacial behavior

Once the cell membrane models have been adequately characterized, studies in curcumin behavior where performed. Fig. 12 shows the resultant curcumin isotherm and its compression modulus, obtained by depositing 85 μl of a 0.5 mg/ml Curc solution.. As can be deduced from its low compressibility modulus (Table 2), curcumin forms a more condensed monolayer at low molecular areas, which barely covers a range of a few tens of $\AA^2$ even though the compression area was the same as for the other isotherms. The incapacity to reach high surface pressures even closing the barriers to the minimum area of the through demonstrates that curcumin experience a low surface activity at the air-water interface . Since the molecular structure contains hydrophilic groups and a hydrophobic region, the disposition of both in the molecule does not confer amphiphilic character.

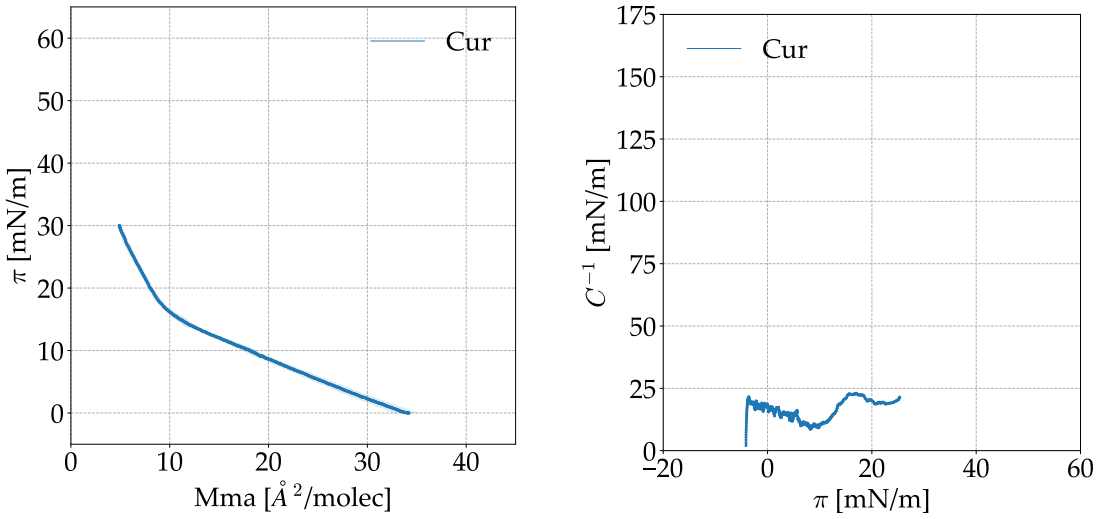

Figure 12: Curcumin isotherm and compression modulus C^{-1} versus surface pressure.

As indicated by the unique maximum of C^{-1} , Curc monolayer undergoes a LE/LC transition and no more phase changes can be observed under these conditions, except for a very small portion of gas phase in the region of larger pressure. Unfortunately, the limited area of the through did not allow to perform a complete isotherm, i.e from the gas phase to collapse, being able to obtain only surface pressures that are far below the reported lateral pressure in cells (30-35 mN/m) [5] . The spreading of a larger volume of solution (a range from 50 μl to 100 μl was tested) caused the isotherm to start in a condensed state where no reference for the surface pressure could be obtained, yielding an invalid measurement. In the next subsection it is explained how the problem of obtaining values at higher pressures in order to analyze its interaction with the membrane models was solved. The characteristic of the curcumin isotherm found here agree with other works results [26]. However, collapsing pressures at about 10.4 mN/m have been reported while in the present work a maximum of 30.54 mN/m has been reached. This discrepancy may arise because Curc can present several arrangements of the atoms within the molecule, what modifies the kind of interaction between the molecules and yields to different results depending on the solution.

In previous sections the data obtained for pure solutions were compared with their corresponding mixed isotherm results. However, it may be interesting to also compare the leading players of the incoming experiments between them. Note that the results obtained ensure the validity of the considered membrane models. Indeed, the smoother curvature of Chol:Sph=0.25 isotherm proves the higher fluidity of the monolayer against the sharper and more compact Chol:DPPC=0.67 film due to, the presence of less cholesterol concentration in the mixture and the chain structure of the Sph, as it was previously mentioned. In addition, the compression modulus of Chol:DPPC=0.67 shows higher values than Chol:Sph=0.25 with a wider C^{-1}_{max}.

In Fig. 13 the isotherms corresponding to the two cell membrane models and curcumin films are presented. From this plot, it can also be seen that both Chol:DPPC=0.67 and Chol:Sph=0.25 present a similar A_0 by analogy to what happened with pure DDCP and Sph due to the "zwitterionic" nature of the DPPC, while the highly condensed Cur

appears at very low areas.

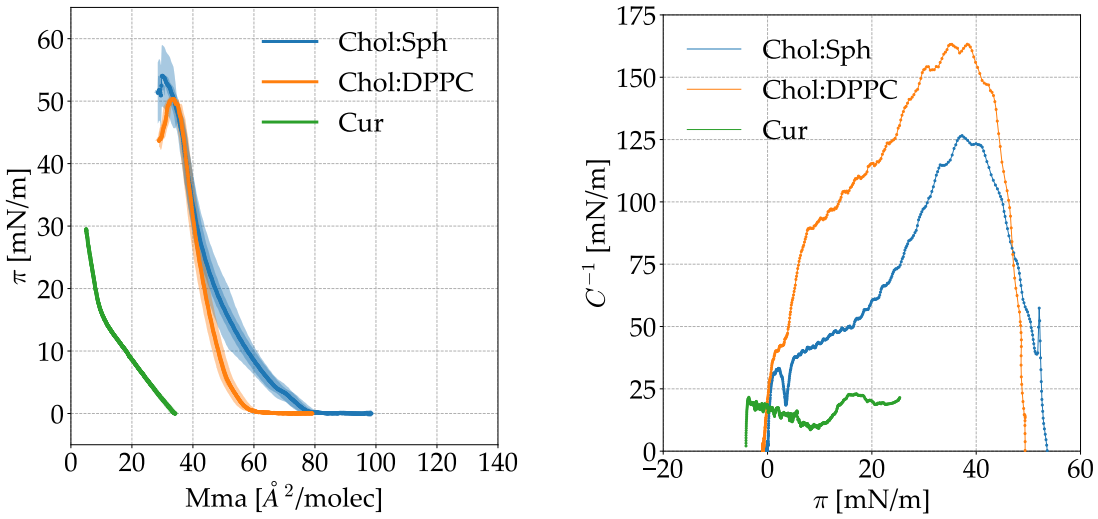

Figure 13: Comparison between the isotherms and compression modulus of pure Curc monolayer and mixed Chol:Sph=0.25 and Chol:DPPC=0.67 films.

	A_0 [$Å^2$/molec]	π_c [mN/m]	C_{cell}^{-1}
Chol:DPPC=0.67	45.23	51.32	268.36
Chol:Sph=0.25	57.21	58.23	62.01
Cur	6.12	-	-

Table 2: Specific limit area A_0, collapse pressure π_c and compression modulus C_{cell}^{-1} at cell membrane lateral pressure for Chol:DPPC=0.67, Chol:Sph=0.25, and pure Cur.

4.5.1 Fit

It was previously discussed that, as curcumin displays a low activity in the air-water interface, the changes in surface pressure observed while compressing where less pronounce, thus it was necessary to cover a larger area with the barriers than allowed by the through in order to see significant changes in the isotherm. As an attempt to address this problem, the curcumin isotherm was fitted with the different models described in Section 2.3.3 with the purpose of extrapolating the high surface pressure regions. All fitting algorithms where previously tested on fully known DPPC isotherms to ensure their correct performance.

Firstly, the models proposed by Fainerman et al. and Brockman et al. (Eq. 2.15 and 2.16 respectively) were tested without conclusive results. Then, the virial expansion given by Eq. 2.11 were fitted up to the fourth, fifth and sixth degree, using both a polinomial and a non linear regression algorithms in Matlab, obtaining values of the χ^2 test around 0.03 in the most favorable cases.

The optimal result had been obtained fitting the model proposed by Birdi et al. [10],which adjust the parameters by means of Eq. 2.14.In order to obtain results with physical mean-

ing, some parameters were initially set in the adjustment process carefully chosen values when the linear regression algorithm was used. Regarding the model suggested by Birdi, A_0 was firstly set as $3\,Å^2/molec$ given the isotherm profiles found in literature [26] and since the incomplete isotherms that could be obtained in the laboratory seem to tend to that specific molecular area at high pressures, and c_1 and c_2 as $40\,mN/m$ and $400\,mN/Å^5$. ϕ_h had been assumed to be 2/3 [10] and an intrinsic parameter of the medium and the component π_{elec} will be negligible given the low electrical charge of curcumin molecules [11], so both were therefore not consider variable parameters in the fitting process. The resultant adjustment parameters and a plot of the fit are shown in Table 3 and Fig. 14. A somewhat lower chi-squared value than in the case of the virial ($\chi^2 = 0.0269$) indicates that this model adjust slighly better to the curcumin isotherm than the virial expansion, the specific area value ($A_0 = 3.425 \pm 0.011 Å^2/molec$) has proven to be similar to the one expected and the negative value of c_2 suggest the presence of attractive van de Waals dispersion forces between the molecules.

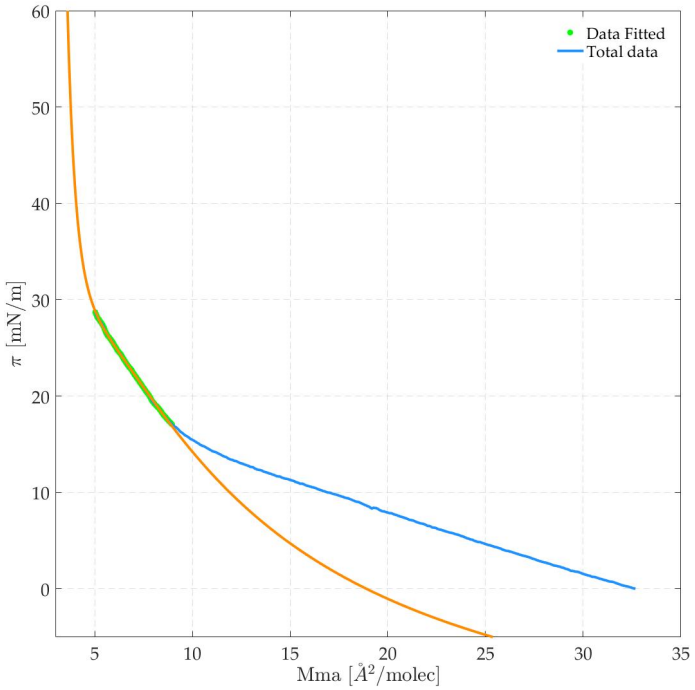

Figure 14: Fitting of the model proposed by Birdi to the curcumin isotherm.

Model	A_0	c_1	c_2	χ^2
Birdi	3.425±0.011$Å^2/molec$	-20.98±0.04 mN/m	-5620±23 $mN/Å^5$	0.02695

Table 3: Final values of the fitting parameters.

4.6 Curcumin-normal cell interaction

Once all the membrane models and the testing drug were fully characterized, curcumin was added to the Chol:DPPC mixed solution in different mole fractions ($\chi_{Cur} = 0; 0.3; 0.5; 0.7; 1.0$). The results of Chol:DPPC mixed films with curcumin added in different mole fractions are represented in Fig. 15.

The analysis of the data presented evidences that the addition of Cur into the systems clearly condenses the mixed monolayer modeling the healthy cell. Increasing the concentration of drug yields to a gradual shift of the Chol:DPPC isotherms towards smaller areas in an extent which nearly follows the same proportion as the molar ratio of Cur. Moreover, the mixed film slightly starts to resemble the steeper curve for one component Cur monolayer.

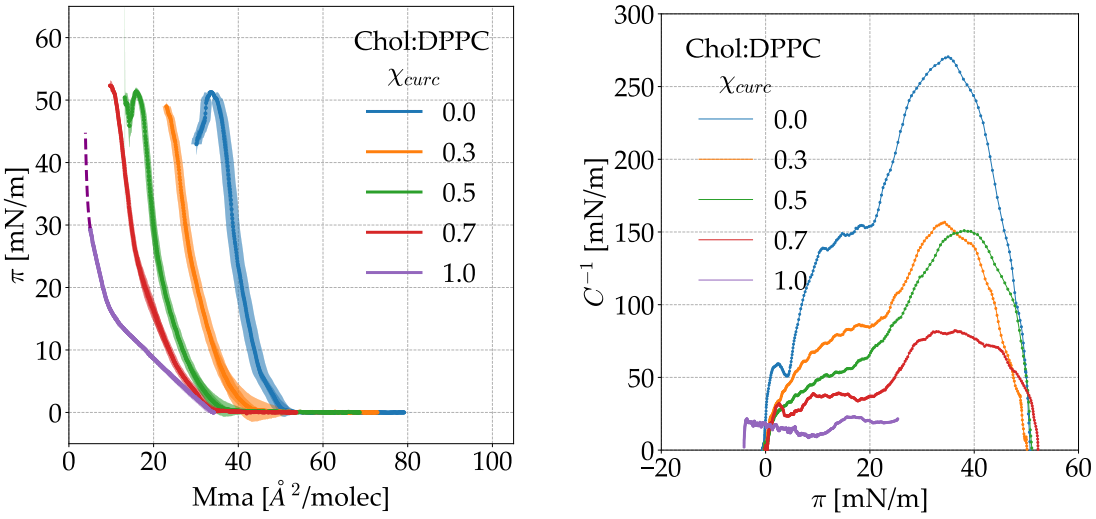

Figure 15: Chol:DPPC isotherms and their compression modulus C^{-1} versus surface pressure for different Cur concentrations.

However, the strong decrease of the compressivity modulus with the increase of curcumine concentration reflects an increase of the fluidity of the film. The maximum decreased and becomes wider and smoother, suggesting that Cur provokes the monolayer to become looser and, at the same time, more condensed. This behavior is due to the fact that curcumin at the air-water interface becames highly condensed at very low molecular area values. This behavior is also reported in systems of DPPC and DPPS monolayers with PMN1 as drug candidate [31].

Chol:DPPC=0.65			
χ_{cur}	A_0 [Å^2/molec]	π_c [mN/m]	C^{-1}_{cell}
0.0	45.23	51.32	268.36
0.3	34.21	51.12	146.20
0.5	23.41	53.01	122.74
0.7	20.74	54.01	81.23
1.0	6.12	-	-

Table 4: Specific limit area A_0, collapse pressure π_c and compression modulus C^{-1}_{cell} at cell membrane lateral pressure of Chol:DPPC=0.65 monolayer at different Cur concentrations.

4.7 Curcumin-tumor cell interaction

Fig. 16 presents the isotherms recorded for Chol:Sph monolayers of various proportion of Cur component and their compression modulus.

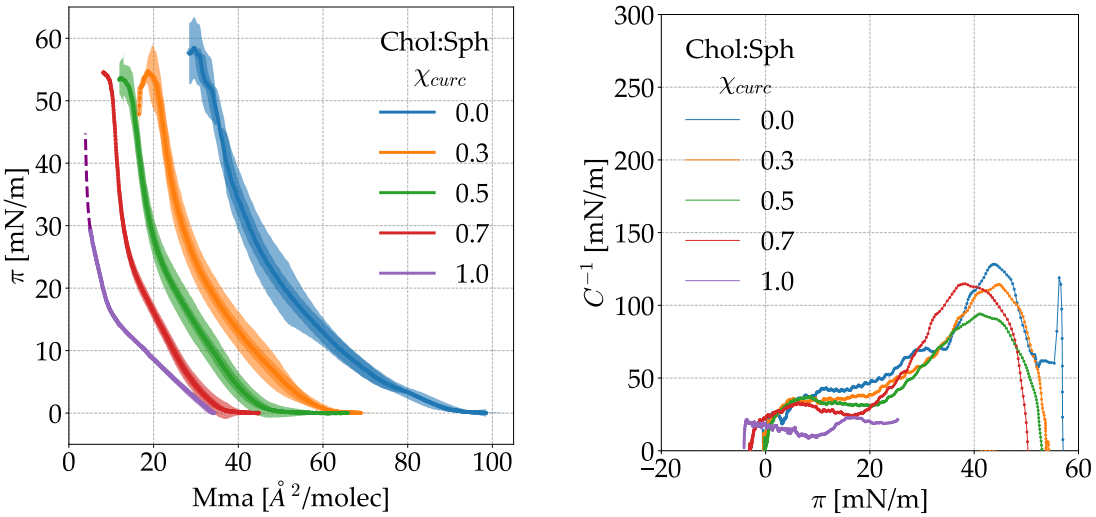

Figure 16: Chol:Sph isotherms and their compression modulus C^{-1} versus surface pressure for different Cur concentrations.

The results suggest that Cur also condenses the tumor cell membrane model toward smaller areas but the changes in the isotherm profile are less obvious than in the previous case. Moreover, C^{-1} does not experience significant changes: the values only decrease (Table 5 and the smoothing is less pronounced than for the Chol:DPPC=0.67 monolayer. In this case the film of Chol:Sph=0.27 is more extended that Chol:DPPC=0.67 monolayer and the condensing effect of curcumin is less pronounced. Even, the LE-LC phase transition does not disappears in all the studied concentration range, therefrom the observed behavior of the compression modulus as a function of the surface pressure.

Chol:Sph=0.25			
χ_{cur}	A_0 [$\AA^2$/molec]	π_c [mN/m]	C^{-1}_{cell}
0.0	57.21	58.23	62.01
0.3	38.47	56.87	55.78
0.5	23.63	54.02	68.45
0.7	15.14	54.78	56.20
1.0	6.12	-	-

Table 5: Specific limit area A_0, collapse pressure π_c and compression modulus C^{-1}_{cell} at cell membrane lateral pressure of Chol:Sph=0.25 monolayer at different Cur concentrations.

4.8 Excess area and Gibbs energy

In order to better understanding the effect of curcumin on cell membrane models, the excess area and excess free energy in function of the curcumin molar fraction have been

studied.

The obtained results of excess area for the tumor and cell membrane models for different proportions of Cur are represented in Fig. 17 and Table 7[3]. For all the studied systems the A_{exc} values were calculated by means of Eq. 2.19 at four different surface pressure covering the LC phase of the isotherms, however, they all were below the collapse pressure for Chol:DDPC and Chol:Sph.

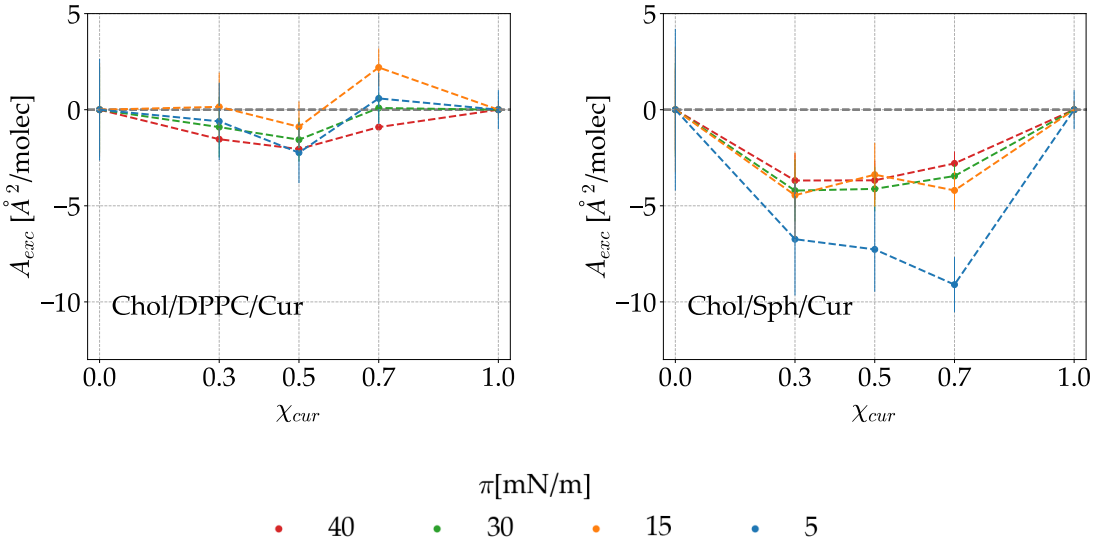

Figure 17: Excess area for Chol:DDPC and Chol:Sph versus Cur concentration.

Chol:DPPC=0.67	A_{exc} [$\mathring{A}^2$/molec]			
χ_{cur}	5	15	30	40
0.0	0.00	0.00	0.00	0.00
0.3	-0.61	0.15	-0.90	1.53
0.5	-2.23	-0.88	-1.55	-2.05
0.7	0.58	2.19	0.08	-0.90
1.0	0.00	0.00	0.00	0.00

Chol:Sph=0.25	A_{exc} [$\mathring{A}^2$/molec]			
χ_{cur}	5	15	30	40
0.0	0.00	0.00	0.00	0.00
0.3	-6.73	-4.44	-4.21	-3.68
0.5	-7.26	-3.37	-4.12	-3.67
0.7	-9.10	-4.20	-3.45	-2.7
1.0	0.00	0.00	0.00	0.00

Table 6: Values of the excess area A_{exc} for different Cur concentrations χ_{cur} and surface pressures π.

The graphs show that for all the mixtures at the studied surface pressures, A_{exc} differs

[3]Errors are of the same order as the values, therefore they are not shown in order not to miss information due to rounding.

from zero, which means non ideal behavior of the film components and thus suggest the arising of interactions between the drug and both membrane models. In addition, the effect of curcumin depends on the proportion of drug added and the surface pressure of the measurement since the amount and distance between molecules determine to a large extent the characteristics of the interactions, as explained throughout this work.

Nevertheless, the more evident deviations from the additivity rule observed for the Chol:Sph system suggest a highly pronounced non ideal behavior and miscibility of the monolayer in the presence of Cur [32]. Furthermore, the values of A_{exc} are more negative than in the healthy membrane model. The strongest interaction (i.e the minimum value of A_{exc}) is reached at $\chi_{Cur} = 0.7$ for $\pi = 5\,mN/m$, but at pressures matching the lateral pressure in cell membranes this minimum shifts to $\chi_{Cur} = 0.3$. This evidences the existence of attractive forces between the drug and the Chol:Sph monolayer that condense the film to a smaller molecular area than the ideal case.

In contrast to the above explained result, deviations from zero for the Chol:DPPC film are less negative, indicating that a more repulsive interaction and low miscibility arise when mixing with curcumin. Furthermore, for $\chi_{Cur} = 0.7$ at 5, 15 and 30 mN/m, and for $\chi_{Cur} = 0.3$ at 30 mN/m, A_{exc} values are slightly positive. This may confirm the existence of repulsive forces between molecules at the interface. The maximum value of the excess area is reached for$\chi_{Cur} = 0.7$ at 15 mN/m and is maintained at pressures similar to that of the cell membranes, the same molar fraction at which the minimum is reached in the previous case, and is maintained at pressures similar to that of the cell membranes.

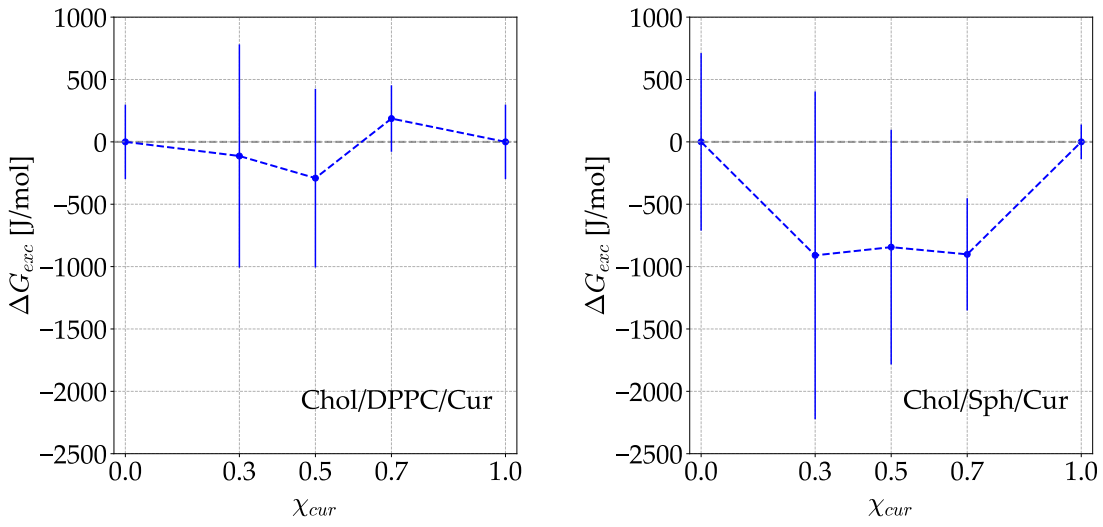

Figure 18: Excess free energy ΔG_{exc} for Chol:DPPC=0.67 and Chol:Sph=0.25 versus Cur concentration.

Chol:DPPC=0.67		Chol:Sph=0.25	
χ_{cur}	ΔG_{exc}[J/mol]	χ_{cur}	ΔG_{exc}[J/mol]
0.0	0.00	0.0	0.00
0.3	-113.35	0.3	-909.83
0.5	-290.62	0.5	-843.97
0.7	186.80	0.7	-901.75
1.0	0.00	1.0	0.00

Table 7: Values of the excess free energy ΔG_{exc} for different Cur concentrations χ_{cur}.

Further information on the miscibility and interactions between the components of the studied mixed films is drawn from the analysis of the excess free energy (Fig. 18). An limit of integration between $5\,mN/m$ and $40\,mN/m$ was set with the purpose of covering the values of membrane lateral pressure in cells. Negative values of ΔG_{exc} for the monolayer of Chol:Sph:Cur indicate that the interactions in the ternary film are stronger than those in the respective binary Chol:Sph and pure Cur monolayers, suggesting a stabilizing effect of the monolayer as they are thermodynamically more favorable[7].

On the other hand, values close to zero found for the Chol:DPPC system indicate that the mixing is closer to ideality and, therefore, incorporation of curcumin causes less disturbance on the system as compared to the effect on the aforementioned monolayer. Particularly, the excess energy display a positive value at $\chi_{Cur} = 0.7$ (Table 7 indicating a particularly low interaction between curcumin molecules and the bicomponent film for that Cur concentration. Chol:Sph shows an almost constant negative value of ΔG_{exc} around . All these results are in accordance with other experiments found in bibliography performed with other drugs and molecular models [3, 19, 7]. These authors concluded that the interactions between both molecules depend on the proportion of the component in the mixed film and on surface pressure values. Only one article [26] have been found where the interaction of curcumin with cell membrane models is analyzed using the Langmuir technique.

Our monolayer experiments show that drug affects both kinds of membranes but it penetrates easier into looser tumor membranes causing stabilization from a thermodynamic point of view. Thus, the healthy cell membrane, which is more condensed, constitutes a natural barrier preventing the drug from incorporating into the membrane. This result shows that curcumin may be a suitable drug candidate for cancer disease and could encourages the use of curcumin as a drug in studies that will be carried out in the future within the framework of the main project aimed at the creation of intelligent nanocapsules for oral administration. This study will be completed by imaging the monolayers for further structural analysis using a Brewster angle microscope as part of an Collaboration Grant.

5 Conclusions

The main conclusions of this Bachelor's final project are presented below:

Regarding my formation, with the fulfillment of this principally experimental project I have learned the use of a complicated experimental technique like the Langmuir film balance, the preparation of solutions and use of material material under extreme cleanliness,

the design of complex experiments at the air-water interface, extraction and management of information from experimental results, the calculation of results by adjusting a theoretical model to experimental results and the use and gathering of specialized research bibliography.

Through this work, surface pressure versus mean molecular area isotherms have been obtained for pure and mixed monolayers formed by DPPC, Shp, Chol and Curc. The values obtained for the parameters characterizing the isotherms and the observed phases are in agreement with bibliographic results. Therefore, it can be considered that the monolayer technique using a Langmuir through have been correctly learned.

A healthy and tumor cell membrane model have been created and characterized using mixed Chol: DDPC and Chol:Sph monolayers, concluding that the addition of cholesterol to the pure films condensate the system and obtaining useful information that will be used in subsequent studies to recreate these models.

Finally, it has been possible to study the interaction of Curc with the aforementioned models, finding that curcumin penetrates more into the tumor cell membrane model, causing its thermodynamic stabilization. This result supports the use of curcumin as a drug candidate in future studies.

6 Acknowledgments

I would like to dedicate this work to my parents and sister, for supporting me through all these hard career years, and to my tutors María José and Julia, thanks for all the knowledge you have shared with me, dedication and time.

References

[1] J. M. Trillo, "Monocapas y multicapas de langsmuir. antecedentes históricos, obtención, caracterización y aplicaciones," in *Monocapas y multicapas de Langsmuir. Antecedentes históricos, obtención, caracterización y aplicaciones*, 1995.

[2] H. Butt, K. Graf, and M. Kappl, *Physics and Chemistry of Interfaces*, ser. Physics textbook. Wiley, 2003. [Online]. Available: https://books.google.es/books?id=r-IpcdGJMJEC

[3] T. M. Nobre, F. J. Pavinatto, L. Caseli, A. Barros-Timmons, P. Dynarowicz-Latka, and O. N. Oliveira, "Interactions of bioactive molecules & nanomaterials with langmuir monolayers as cell membrane models," *Thin Solid Films*, vol. 593, pp. 158 –188, 2015. [Online]. Available: http://www.sciencedirect.com/science/article/pii/S0040609015009256

[4] "Wikipedia-surfactant," Jun. 2018. [Online]. Available: https://en.wikipedia.org/wiki/Surfactant

[5] D. Marsh, "Lateral pressure in membranes," *Biochimica et Biophysica Acta (BBA) - Reviews on Biomembranes*, vol. 1286, no. 3, pp. 183 – 223, 1996. [Online]. Available: http://www.sciencedirect.com/science/article/pii/S0304415796000093

[6] H. Brockman, "Lipid monolayers: why use half a membrane to characterize protein-membrane interactions," *Current Opinion in Structural Biology*, vol. 9, no. 4, pp. 438 – 443, 1999. [Online]. Available: http://www.sciencedirect.com/science/article/pii/S0959440X9980061X

[7] K. Hac-Wydro and P. Dynarowicz-Latka, "Effect of edelfosine on tumor and normal cells model membranes—a comparative study," *Colloids and Surfaces B: Biointerfaces*, vol. 76, no. 1, pp. 366 – 369, 2010. [Online]. Available: http://www.sciencedirect.com/science/article/pii/S0927776509004974

[8] M. Inbar, R. Goldman, L. Inbar, I. Bursuker, B. Goldman, E. Akstein, P. Segal, E. Ipp, and I. Ben-Bassat, "Fluidity difference of membrane lipids in human normal and leukemic lymphocytes as controlled by serum components," *Cancer Research*, vol. 37, no. 9, pp. 3037–3041, 1977. [Online]. Available: http://cancerres.aacrjournals.org/content/37/9/3037

[9] M. J. Gálvez-Ruiz, "Termodinamica de los cambios de fase en monocapas simples y mixtas de colesterol -lx-fosfatidilcolina-acidos biliares," Ph.D. dissertation, Universidad de Granada, 1988.

[10] K. S. Birdi, F. Madsen, and K. Eberth, "Determination of van der waals forces in monolayer films of lipids & biopolymers. equation of state for two-dimensional films," *Colloid and Polymer Science*, vol. 272, no. 8, pp. 1000–1004, Aug 1994. [Online]. Available: https://doi.org/10.1007/BF00658899

[11] J. Sánchez-González, M. Cabrerizo-Vílchez, and M. Gálvez-Ruiz, "Evaluation of the interactions between lipids and γ-globulin protein at the air–liquid interface," *Colloids and Surfaces B: Biointerfaces*, vol. 12, no. 3, pp. 123 – 138, 1999. [Online]. Available: http://www.sciencedirect.com/science/article/pii/S0927776598000691

[12] V. B. Fainerman and D. Vollhardt, "Equations of state for langmuir monolayers with two-dimensional phase transitions," *The Journal of Physical Chemistry B*, vol. 103, no. 1, pp. 145–150, 1999. [Online]. Available: https://doi.org/10.1021/jp983109q

[13] J. M. Smaby and H. L. Brockman, "Characterization of lipid miscibility in liquid-expanded monolayers at the gas-liquid interface," *Langmuir*, vol. 8, no. 2, pp. 563–570, 1992. [Online]. Available: https://doi.org/10.1021/la00038a042

[14] Albrecht, O., Gruler, H., and Sackmann, E., "Polymorphism of phospholipid monolayers," *J. Phys. France*, vol. 39, no. 3, pp. 301–313, 1978. [Online]. Available: https://doi.org/10.1051/jphys:01978003903030100

[15] J. Sánchez-González, "Estudio termodinámico de un sistema bidimensional: Monocapas de lípidos," mathesis, Universidad de Granada, 1993.

[16] D. Myers, *Surfaces, Interfaces, and Colloids: Principles and Applications*. Wiley, 1991. [Online]. Available: https://books.google.es/books?id=UdgsAAAACAAJ

[17] J. Sánchez-González, "Investigación del comportamiento interfacial de lípidos y proteínas. formación y caracterización de películas monomoleculares," Ph.D. dissertation, Universidad de Granada, 1999.

[18] R. Maget-Dana, "The monolayer technique: a potent tool for studying the interfacial properties of antimicrobial and membrane-lytic peptides and their interactions with lipid membranes," *Biochimica et biophysica acta*, vol. 1462, no. 1-2, p. 109—140, December 1999. [Online]. Available: https://doi.org/10.1016/S0005-2736(99)00203-5

[19] K. Hac-Wydro, P. Dynarowicz-Latka, P. Wydro, and K. Bak, "Edelfosine disturbs the sphingomyelin-cholesterol model membrane system in a cholesterol-dependent way-the langmuir monolayer study," *Colloids and Surfaces B: Biointerfaces*, vol. 88, no. 2, pp. 635 – 640, 2011. [Online]. Available: http://www.sciencedirect.com/science/article/pii/S0927776511004589

[20] "Pubchem - open chemistry database," May 2018. [Online]. Available: https://pubchem.ncbi.nlm.nih.gov/

[21] "Wikipedia-tensioactive," Jun. 2018. [Online]. Available: https://en.wikipedia.org/wiki/Zwitterion

[22] "Avanti - polar lipids, inc." [Online]. Available: https://avantilipids.com/

[23] "Sigma-aldrich, inc." Mar. 2018. [Online]. Available: https://www.sigmaaldrich.com/united-states.html

[24] X.-M. Li, J. M. Smaby, M. M. Momsen, H. L. Brockman, and R. E. Brown, "Sphingomyelin interfacial behavior: The impact of changing acyl chain composition," *Biophysical Journal*, vol. 78, no. 4, pp. 1921 – 1931, 2000. [Online]. Available: http://www.sciencedirect.com/science/article/pii/S0006349500767403

[25] A. K. BHARAT B. AGGARWAL and A. C. BHARTI, "Anticancer potential of curcumin: Preclinical and clinical studies," *ANTICANCER RESEARCH*, vol. 23, pp. 363–398, 2003.

[26] A. Karewicz, D. Bielska, B. Gzyl-Malcher, M. Kepczynski, R. Lach, and M. Nowakowska, "Interaction of curcumin with lipid monolayers and liposomal bilayers," *Colloids and Surfaces B: Biointerfaces*, vol. 88, no. 1, pp. 231 – 239, 2011. [Online]. Available: http://www.sciencedirect.com/science/article/pii/S0927776511003869

[27] "Ksv instruments ltd: Langmuir & langmuir-blodgett troughs." [Online]. Available: https://www.biolinscientific.com/ksvnima/fabrication-and-characterization-of-thin-films/langmuir-and-langmuir-blodgett-troughs

[28] L. P. A.F. Mingotaud, C. Mingotaud, *Hanbbook of Monolayers*. Academic Press Inc., 1993.

[29] M. Gálvez-Ruiz and M. A. Cabrerizo Vílchez, "A study of the miscibility of bile components in mixed monolayers at the air-liquid interface i. cholesterol, lecithin, and lithocholic acid," vol. 269, pp. 77–84, 01 1991.

[30] C. O'Connor and R. Wallace, "Bile salt micelles," *Adv. Colloid Interface Sci.*, vol. 22, no. 1, 1985.

[31] L. F. G. Salis, G. N. Jaroque, J. F. B. Escobar, C. Giordani, A. M. Martinez, D. M. M. Fernández, F. Castelli, M. G. Sarpietro, and L. Caseli, "Interaction of 3′,4′,6′-trimyristoyl-uridine derivative as potential anticancer drug with phospholipids of tumorigenic and non-tumorigenic cells," *Applied Surface Science*, vol. 426, pp. 77 – 86, 2017. [Online]. Available: http://www.sciencedirect.com/science/article/pii/S0169433217320846

[32] K. Weder, M. Mach, K. Hac-Wydro, and P. Wydro, "Studies on the interactions of anticancer drug - minerval - with membrane lipids in binary and ternary langmuir monolayers," *Biochimica et Biophysica Acta (BBA) - Biomembranes*, 2018. [Online]. Available: http://www.sciencedirect.com/science/article/pii/S0005273618301615